

## Quantization of the coupling mechanism between eco-environmental quality and urbanization from multisource remote sensing data

Dong Xu<sup>a,b,1</sup>, Feng Yang<sup>a,b,1,\*</sup>, Le Yu<sup>c,d</sup>, Yuyu Zhou<sup>e</sup>, Haixing Li<sup>f</sup>, Jinji Ma<sup>g</sup>, Jincai Huang<sup>h</sup>, Jing Wei<sup>i</sup>, Yang Xu<sup>j</sup>, Chong Zhang<sup>k</sup>, Jie Cheng<sup>a,b</sup>

<sup>a</sup> State Key Laboratory of Remote Sensing Science, Faculty of Geographical Science, Beijing Normal University, Beijing, 100875, China

<sup>b</sup> Institute of Remote Sensing Science and Engineering, Faculty of Geographical Science, Beijing Normal University, Beijing, 100875, China

<sup>c</sup> Ministry of Education Key Laboratory for Earth System Modeling, Department of Earth System Science, Tsinghua University, Beijing, 100084, China

<sup>d</sup> Ministry of Education Ecological Field Station for East Asia Migratory Birds, Tsinghua University, Beijing, 100084, China

<sup>e</sup> Department of Geological and Atmospheric Sciences, Iowa State University, Ames, IA, 50011, USA

<sup>f</sup> College of Geomatics Science and Technology, Nanjing Tech University, Nanjing, 211816, China

<sup>g</sup> School of Geography and Tourism, Anhui Normal University, Wuhu, 241002, China

<sup>h</sup> Shenzhen Key Laboratory of Spatial Smart Sensing and Service, Shenzhen University, Shenzhen, 518060, China

<sup>i</sup> Department of Chemical and Biochemical Engineering, Iowa Technology Institute, University of Iowa, Iowa City, IA, 52242, USA

<sup>j</sup> The College of Environment and Planning, Henan University, Kaifeng, 475004, China

<sup>k</sup> Shaanxi Key Laboratory of Disaster Monitoring and Mechanism Modeling, Baoji University of Arts and Sciences, Baoji, 721013, China

### ARTICLE INFO

Handling editor: M.T. Moreira

#### Keywords:

Eco-environment quality

Urbanization

Coupling coordination degree

Sustainable development goals

Central and eastern regions of China

### ABSTRACT

The rapid urbanization in central and eastern China has posed a major threat to the green sustainable development of the ecological environment. However, the understanding of the interactive coupling mechanism between urbanization and eco-environmental quality (EEQ) remains to be developed. Understanding their interactive coupling mechanism is of great significance to achieve the urban sustainable development goal. By using multi-source remote sensing data, we intended to answer "What are the temporal and spatial characteristics of urbanization and EEQ in the central and eastern regions of China on the pixel scale in the past 24 years, and what is the coupling mechanism between the urbanization and the EEQ?". To answer these questions, we improved a pixel-based model (i.e., RSEI-2) to assess the EEQ in China and explored the coupling mechanism between the urbanization and the EEQ in central and eastern China with the combination method of mathematics and graphics. The results showed that the urbanization and the coupling coordination degree (CCD) of the whole region continually increased from 1992 to 2015, especially in the three major urban agglomerations. The CCD of the provinces in these regions exhibited a strong spatial dependence, with the spatial distribution pattern of "low inside, high outside, high in the east and low in the west". The EEQ did not change significantly, whilst the three major urban agglomerations showed a significant downward trend. Most importantly, this study found that the urbanization determined the development of the CCD lying within the critical value. In addition, the improved RSEI-2 in this study provided great convenience for monitoring the EEQ in China. This study fills the gap in studying the interaction mechanism between the urbanization and the EEQ, and also provides a new perspective for the research on the urban sustainable development in China and even the world.

### 1. Introduction

As the largest developing country worldwide, China has been experiencing an unprecedented urbanization development process since the establishment of the socialist market economic system (Dou and Kuang, 2020). Especially, in the central and eastern regions of China, the

population of these regions accounts for about 98% of the total population of China, and the proportion of GDP represents about 87% (National Bureau of Statistics, <http://www.stats.gov.cn/>). The rapid urbanization has played an important role in reducing the number of people in poverty, promoting economic growth (Henderson, 2003), and improving social living standards (Capps et al., 2016) of the region. Simultaneously, the rapid increase in the population density and

\* Corresponding author. State Key Laboratory of Remote Sensing Science, Faculty of Geographical Science, Beijing Normal University, Beijing, 100875, China.  
E-mail address: [yftaurus@mail.bnu.edu.cn](mailto:yftaurus@mail.bnu.edu.cn) (F. Yang).

<sup>1</sup> Dong Xu and Feng Yang contributed equally to this work.

excessive resource consumption have also caused a series of ecological and environmental problems, such as land degradation (Abu Hammad

## Abbreviations

EEQ	eco-environmental quality
CCDM	coupling coordination degree model
CCD	coupling coordination degree
RSEI	remote sensing ecological index
RSEI-2	remote sensing ecological index-2
GEE	Google Earth Engine.

and Tumeizi, 2012), water shortages (Oo et al., 2020), species extinction (McKinney, 2008), frequent natural disasters (Gu et al., 2011), and damage to ecosystem services (MafiGholami and Baharlouii, 2019). These have been posing a major challenge to achieving the urban sustainable development goal (Jalil et al., 2020). However, the coupling mechanism between the eco-environmental quality (EEQ) and the urbanization remains to be understood. Therefore, scientific methods are urgently needed to quantitatively explore the coupling mechanism between the EEQ and the urbanization in the central and eastern regions of China in the past few decades. In order to provide a scientific reference for urban planners to formulate universal urban development strategies and thus alleviate the potential ecological risks induced by the accelerated urbanization development in the future (Kong et al., 2014; Grilo et al., 2020).

As one of the international hotspots in the field of earth science and sustainable development science, the research on the interaction and coupling mechanism of the EEQ and the urbanization has made great progress (Fang et al., 2017; Fan et al., 2020). Currently, related theories and methods include the environmental Kuznets curve (EKC) (Fang et al., 2015), the planetary boundaries theory (Fanning et al., 2020), the tele-coupling theory (Fang and Ren, 2017), the footprint family theory (Yang and Meng, 2019), the urban metabolism theory (Beloin-Saint-Pierre et al., 2017), the STIRPAT model (Yang et al., 2018), the coupling coordination degree model (CCDM) (Song et al., 2018) and the multi-agent model (Yan et al., 2018). Among them, EKC and CCDM are the most widely used models. EKC shows that the urbanization has a non-linear impact on the ecological environment, and numerous studies have also proved this hypothesis (Chikaraishi et al., 2015; Zhao et al., 2016; Martínez-Zarzoso and Maruotti, 2011). However, some scholars pointed out that the EKC theory was not applicable to all countries, especially developing countries (Zhao et al., 2016; Geng and Zhang, 2020). The main reason is that the EKC theory believes the environment and urbanization are independent of each other (Liu et al., 2018a), and only considers the impact of urbanization on the environment regardless of the environmental effects on the urbanization (Cui et al., 2019).

Compared with EKC, the CCDM focuses more on describing the interaction between two or more subsystems (Fu et al., 2020), which can well explain the sustainable development of systems (Fan et al., 2019; Cai et al., 2021). At present, numerous scholars have conducted various studies about China based on the CCDM (Fang et al., 2016). For example, Zhang et al. (Zhang and Li, 2020) studied the coupling relationship between the urbanization and geological disasters over the past two decades and found that the overall coupling degree of the urbanization and the geological disasters exhibited a continuous upward trend in a U-form. Chen et al. (2020) analyzed the coupling relationship between the carbon emissions and the EEQ during 2009–2015 and found that the carbon emissions had a positive effect on the CCD increase, whilst the EEQ determined the direction of the coordinated development. Liu et al. (2018b) evaluated the CCD status between the urbanization and the EEQ in 30 provinces of China during 2005–2015 and found that the coupling

status gradually improved, which was in line with Lu's study (Lu et al., 2019). However, through investigation and summary, it is found that the existing relevant studies still have many limitations.

Firstly, most studies used statistical data as the input parameters of the model, resulting in a rough spatial resolution of the research results which cannot reflect pixel-level spatial information (Liang et al., 2019). Multi-source statistical data can also lead to extremely uncertain results (Shao et al., 2020). Secondly, the existing studies are mainly carried out on the local scale, and the evaluation system lacks a unified standard, integrity and systematicness (Chen et al., 2020; Feng et al., 2021). Specifically, most of them often take cities (He et al., 2017), urban agglomerations (Fang et al., 2019) and watersheds (Liu et al., 2021) as the study units, which hinders the horizontal comparison of different study areas and cannot provide a scientific reference for the sustainable development of areas beyond the study area. In addition, the existing studies on the coupling between the EEQ and the urbanization still focus on the result analysis, and thus this causes the unclear coupling mechanism between the EEQ and the urbanization (Fang and Wang, 2013).

Currently, the rapid development of remote sensing technologies and the open access of multi-source remote sensing data have greatly promoted the earth observation research on the regional scale, which also provides a new method for regional EEQ monitoring and urbanization assessment (Shao et al., 2020; Zheng et al., 2020a). For example, Xu (2013a) proposed a remote sensing-based EEQ evaluation model (RSEI) in 2013, which is widely used for regional EEQ monitoring due to its simplicity and reliability (Shan et al., 2019; Guo et al., 2020). However, the RSEI is only applicable to the urban ecological environment quality monitoring, and the accuracy of the EEQ monitoring throughout China is low (Xu, 2013b). Furthermore, the advantages of nighttime light data in characterizing the level of urbanization have been verified (Zheng et al., 2020a; Chen et al., 2003).

The emergence of remote sensing has effectively solved the first shortcoming of the above. However, no studies can completely overcome the remaining three shortcomings. Therefore, in order to provide a scientific reference for planners to formulate universal urban development strategies, a pixel-based model (i.e., RSEI-2) applicable to the regional EEQ monitoring in China is proposed. Thus, the potential ecological risks due to the accelerated urbanization development in the future can be mitigated. Based on the RSEI-2, CCDM and multi-source remote sensing data, this study explores the coupling mechanism between the EEQ and the urbanization in central and eastern regions of China from 1992 to 2015. The main purpose of this paper is to: 1) explore the coupling mechanism of the EEQ and the urbanization in the central and eastern regions of China on the pixel scale, 2) explore the characteristics of temporal and spatial changes and distribution patterns of the EEQ, the urbanization, and the coupling coordination degree (CCD) in the central and eastern regions of China over the past 24 years, 3) improve the RSEI model and establish a regional EEQ assessment model applicable to China. This study overcomes the shortcomings in the existing research and also fills the gaps among the research on the coupling mechanism between the EEQ and the urbanization.

This article is organized as follows: following the Introduction, Section 2 describes the study area and data, Section 3 introduces the research methods, Section 4 presents the results and discussion, Section 5 demonstrates the coupling coordination mechanism and simulates future coupling coordination degree, and Section 6 summarizes this research.

## 2. Study area and data

### 2.1. Study area

Relying on natural geographical advantages, China's central and eastern regions' economy (except for Xinjiang Uygur Autonomous Region, Tibet Autonomous Region, and Qinghai Province) has experienced rapid economic growth, rapid population growth, and continuous

urbanization during 1992–2015. Simultaneously, the eco-environment problems during the regional development process are not optimistic. Therefore, this study takes the central and eastern regions of China as the study area to explore the coupling mechanism between the EEQ and urbanization.

The study area is bordered by the East China Sea in the east, the South China Sea in the south, the three provinces of Xin-Qing-Xi in the west, and Mongolia and Russia in the north (Fig. 1). The study area has a rich ecosystem, e.g., three major forestry districts of China (Bai et al., 2018). Additionally, there are three characteristic features in nature aspects: the Inner Mongolia Plateau contains the richest grassland resources in China (Wang et al., 2017a); the North China Plain and the Middle and Lower Yangtze River Plains, as important grain producing areas in China, provide a rich farmland ecosystem (Wang et al., 2017b); and in addition to the large and small lakes, constitute the rich and complex wetland ecosystem (Mao et al., 2018), as well as two important ecological barriers in China, the Yangtze River and the Yellow River, that play an important role in maintaining biodiversity, alleviating water shortages, flood control, and irrigation (Yu et al., 2018). In addition, the study area includes three major urban agglomerations, i.e., the Yangtze River Delta urban agglomerations with the most economically dynamic resource allocation center, the Beijing-Tianjin-Hebei urban agglomerations in the national ecological restoration and environmental improvement demonstration zone, and the Pearl River Delta urban agglomerations in the pioneering area of China's open innovation. The three urban agglomerations are becoming the pioneers of China's sustainable development. As of 2019, this study area has 97.59% in the proportion of China's total population, and it is 87.27% in China's GDP proportion (National Bureau of Statistics, <http://www.stats.gov.cn/>).

## 2.2. Study data

The researchers of this study mainly collected the administrative division data (National Earth System Sci), Landsat surface reflectance data, MOD09A1 surface reflectance data, MOD11A2 land surface temperature data, the national county Ecological Index (EI) data, the nighttime light data from DMSP/OLS and VIRRS-NPP, the land use and land cover data (LULC), and 1-km national population density data (POP) during 2015. Here, the administrative division data are downloaded from the National Catalogue Service for Geographic Information; the Landsat and MODIS data is downloaded from the National Aeronautics and Space Administration; the EI data is provided by the Ministry of Ecology and Environment of the People's Republic of China; the nighttime light data is obtained from Zhou's paper (Li et al., 2020); the LULC data is available from Yu's paper (Xu et al., 2020), and the POP data is downloaded from Resource and Environment Science and Data Center. More detailed information about these data can be described in Table 1.

## 3. Methods

Fig. 2 displays the framework for calculating CCD in this study, and the detailed steps are as follows: (1) we performed preprocessing of cloud removal, splicing, striping, clipping, synthesis and resampling (1 km) on the Landsat image data; (2) we calculated greenness (NDVI) (Tucker, 1979), dryness (NDBSI) (Rikimaru et al., 2002), heat (LST) (Ermida et al., 2020), and humidity (WET) (Crist, 1985) indexes based on the preprocessed annual average Landsat surface reflectance data, and also calculated the above four indexes using the MODIS data, which are used to fill in missing values for the Landsat pixels; (3) we calculated the abundance index of land cover types (LCTAI) in the study area from

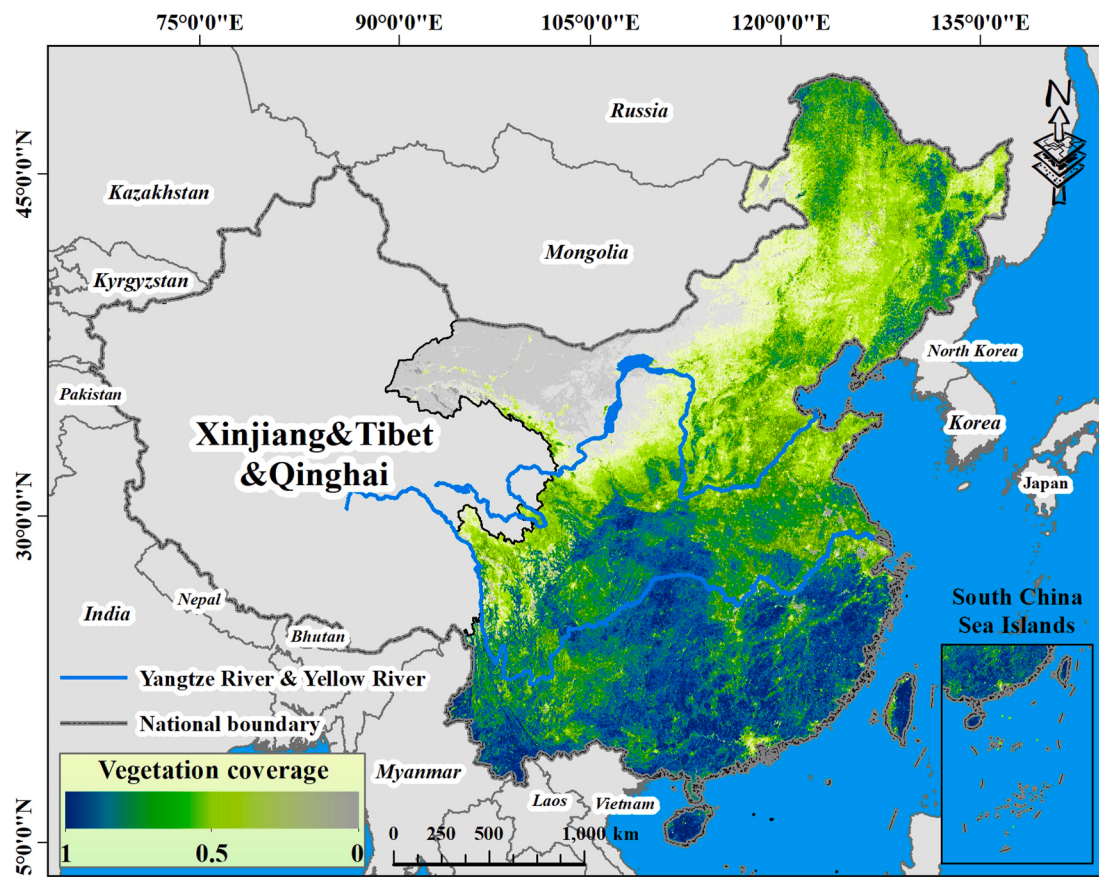


Fig. 1. Spatial location map of the study area.

**Table 1**

The detailed descriptions of the study data.

Data name	Spatial resolution	Time resolution	Source	Function
The administrative division data	1: 1 million	2015	NCSFGI. <sup>a</sup>	Use basic base map data and perform zonal statistics
Landsat5, 7, and 8	30 m	16-Day	USGS. <sup>b</sup>	Calculate the E index
MOD09A1	500 m	8-Day	USGS. <sup>b</sup>	Calculate the E index
MOD11A2	1000 m	8-Day	USGS. <sup>b</sup>	Fill missing LST for Landsat pixels
EI	County unit	2015	MEEPBC <sup>c</sup>	Evaluate RSEI and RSEI-2 indexes
The nighttime light data	1000 m	Annual	Paper (Li et al., 2020)	Calculate the U index
LULC	1000 m	Annual	Paper (Xu et al., 2020)	Calculate the AI index
The POP. data	1000 m	2015	RESDC. <sup>d</sup>	Divide the cities into different sizes

<sup>a</sup> National Catalogue Service for Geographic Information. (<https://www.webmap.cn/>).<sup>b</sup> United States Geological Survey. (<https://earthexplorer.usgs.gov/>).<sup>c</sup> Ministry of Ecology and Environment of the People's Republic of China. (<http://www.mee.gov.cn/>).<sup>d</sup> Resource and Environment Science and Data Center.

1992 to 2015 based the LULC data referring to the “Technical Criterion for Ecosystem Status Evaluation” (192-2015 and Technical Cr, 2015); (4) the five calculated indexes, sequentially were standardized, synthesized, and executed the principal component analysis (PCA), and the PC1 band was the EEQ index, namely RSEI-2 after the PCA operation; and (5) the CCD data between the EEQ and urbanization in the study area during 1992–2015 was obtained when the RSEI-2 and the nighttime light data were added into the CCD model after the consistency processing.

### 3.1. Evaluation of the eco-environment quality

On the basis of the original RSEI model, this study developed a new EEQ evaluation model for remote sensing data, namely RSEI-2 at the regional scale:

$$RSEI_{-2} = \frac{PC1 - PC1_{\min}}{PC1 - PC1_{\max}} \quad (1)$$

$$PC1 = PCA(NDVI, NDBSI, LST, WET, AI) \quad (2)$$

where RSEI-2 was the EEQ index, PC1 was the first principal component,  $PC1_{\min}$  was the minimum value of PC1,  $PC1_{\max}$  was the maximum value of PC1, and NDVI, NDBSI, LST, WET, and AI were greenness, dryness, heat, humidity, and abundance index for land cover type, respectively. The traditional RSEI model was often used to monitor the EEQ at the local scale. Additionally, a small number of scholars (Liao and Jiang, 2020) adopted the RSEI model to evaluate the China's EEQ, but none of them considered the RSEI model's applicability at the regional scale. The results caused significant problems for the research conclusions. Therefore, this study improved RSEI, i.e., RSEI-2 and then evaluated the applicability of the RSEI and RSEI-2 models in China. The results are shown in section 4.1.

Specifically, the EI index calculation greatly depended on the abundance index of land cover types, while four of the aforementioned indexes in the RSEI model did not involve the important evaluation factor. Therefore, after referring to the “Technical Criterion for Ecosystem Status Evaluation” (192-2015 and Technical Cr, 2015), we calculated the abundance index for land cover types (AI) in the study area during 1992–2015 based on the LULC data. The AI was calculated as follows:

$$AI = \mu \times (0.35 \times Forest + 0.21 \times Grassland + 0.28 \times Water + 0.11 \times Cropland + 0.04 \times Built + 0.01 \times Unused) / Area \quad (3)$$

where AI was the abundance index for land cover types,  $\mu$  was the normalized coefficient, Forest, Grassland, Water, Cropland, Built, and Unused were the area of forest land, grassland, waterbody, cropland, built-up, and unused land, respectively, and Area was the total area of the statistical area.

The land surface temperature (LST) index was calculated from the open-source code (the SMW algorithm) provided by Ermida et al. (2020)

at the Google Earth Engine (GEE) platform (Gorelick et al., 2017). Additionally, the WET index calculation for the MODIS data referred to the Index DataBase (<https://www.indexdatabase.de/>). The WET index was calculated as follows:

$$WET_{MODIS} = 0.1509 \times Blue + 0.1973 \times Green + 0.3279 \times Red + 0.3406 \times NIR - 0.7112 \times SWIR1 - 0.4572 \times SWIR2 \quad (4)$$

where  $WET_{MODIS}$  was the WET index, Blue, Green, Red, NIR, SWIR1, and SWIR2 were the blue, green, red, near-infrared, short-wave infrared 1, and short-wave infrared 2 bands for MOD09A1 data, respectively.

### 3.2. Evaluation of urbanization

Numerous scholars have quantitatively evaluated urbanization using remote sensing data. Among them, the CNLI model proposed by Chen et al. (LiShi and Jin, 2003) was widely used in the regional urbanization monitoring. The CNLI model reflects the urbanization level of the area at two attributes: the average light intensity and the light area. The CNLI was calculated as follows:

$$CNLI = I \times S \quad (5)$$

$$I = \sum_{i=1}^{63} DN_i \times \frac{n_i}{N \times 63} \quad (6)$$

$$S = \frac{Area_N}{Area} \quad (7)$$

where CNLI was the urbanization index,  $I$  was the average light intensity,  $S$  was the light area,  $DN_i$  was the light gray value of the  $i$ -th level,  $n_i$  was the number of pixels of the  $i$ -th level gray value,  $N$  was the total number of the light pixels,  $Area_N$  was the total area of the light pixels, and  $Area$  was the total area.

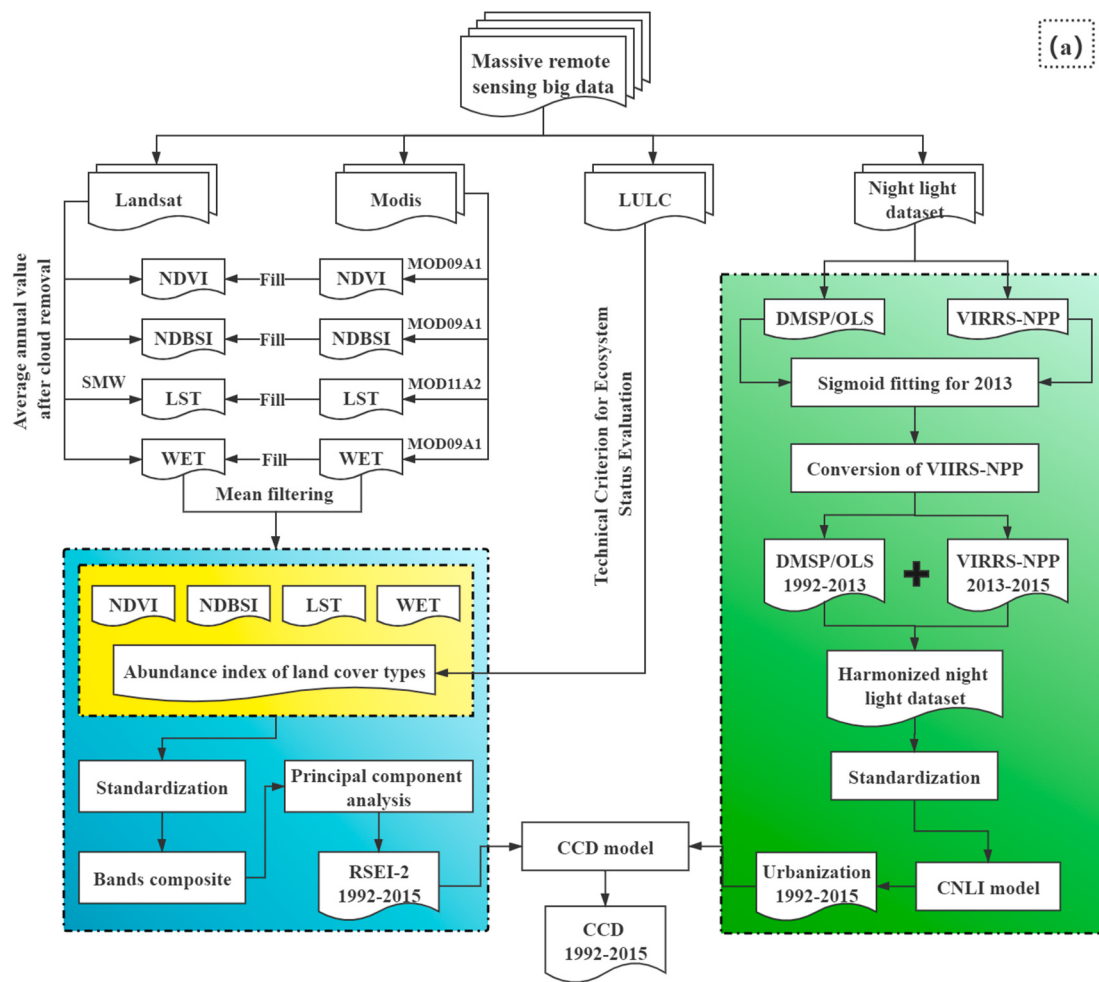
### 3.3. The CCD model

The CCD between the EEQ and urbanization determined the urban sustainable development's direction (Seto et al., 2010). This study explored the coupling mechanism between the EEQ and urbanization in the central and eastern regions of China using the CCD model. The CCD model was calculated as follows:

$$C = \left\{ \frac{U \times E}{[(U + E)/2]^2} \right\}^{\frac{1}{2}} \quad (8)$$

where  $C$  was the coupling degree between the EEQ and urbanization,  $C$  ranged from 0 to 1,  $U$  was the urbanization index, namely CNLI, and  $E$  was the EEQ index, namely RSEI-2.

In order to avoid the phenomenon of “the false coordination”, that is, the phenomenon that  $U$  and  $E$  were both low but  $C$  was high, the CCD model was improved on the basis of the coupling degree:



Example for 2015:

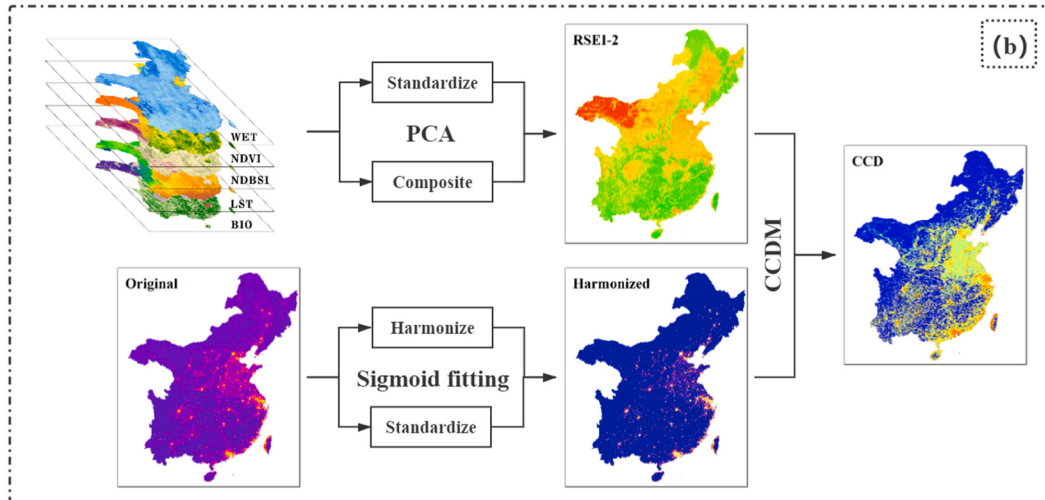


**Fig. 2.** The technology roadmap for this study. (a) The framework for evaluating the coupling coordination degree (CCD): the content in the yellow area is to obtain the eco-environment evaluation index, the content of the light blue area is to calculate the RSEI-2, and the content of the light green area is processing processes for the nighttime light data; (b) a case for calculating the CCD during 2015. The standard of standardization in this study is to take the maximum and minimum values of all data of each index from 1992 to 2015 as the standardized extreme values.

$$D = \sqrt{C \times T} \quad (9)$$

$$T = \alpha U + \beta E \quad (10)$$

where  $D$  was the CCD ranging from 0 to 1 where the higher  $D$  indicated

the higher the level of coordinated development between EEQ and urbanization,  $T$  was the comprehensive evaluation index of  $U$  and  $E$ ,  $\alpha$  and  $\beta$  were the weights of  $U$  and  $E$ , respectively, where  $\alpha + \beta = 1$ . Because the EEQ and urbanization had the same interaction,  $\alpha$  and  $\beta$  were set as 0.5 in this study, respectively.

### 3.4. The trend analysis method

This study quantified the time change rate of the EEQ, urbanization, and the CCD in this study during 1992–2015 using the trend analysis method (Tian et al., 2015). The calculation formula was as follows:

$$\text{Slope} = \frac{n \times \sum_{i=1}^n i \times Y_i - \sum_{i=1}^n i \sum_{i=1}^n Y_i}{n \times \sum_{i=1}^n i^2 - (\sum_{i=1}^n i)^2} \quad (11)$$

where  $n$  was the number of years and was set to 24 in this paper,  $i$  was the serial number of the year,  $Y_i$  was the Y index value of the  $i$ -th year, and slope was the slope of the index change where when slope was positive, the index will present an increasing trend; on the contrary, it will have a downward trend.

## 4. Results

### 4.1. Regional adaptation assessment of RSEI and RSEI-2

Using the method in Section 3.1, we calculated the RSEI and RSEI-2 values of each district and county's study area and then evaluated the RSEI and RSEI-2's regional adaptability compared to the EI data (see Fig. 3). We found from Fig. 3 (left) that the RSEI index was significantly underestimated from the bias value and the deviation between the fitting line and the 1:1 line, and the underestimation degree could reach 24%. Additionally, the RSEI was reasonable to some extent in terms of the RMSE (0.27 [27%]) and the  $R^2$  (0.55). However, the proposed RSEI-2 model improved underestimation phenomenon using the original model (Fig. 3 right), and the degree of underestimation decreased from 24% to 5%. The RSEI-2's accuracy had also significantly improved with an RMSE of 0.11 (11%) and  $R^2$  of 0.71. This suggested that the RSEI-2 model's accuracy was better than that of the RSEI model for monitoring EEQ at the national regional scale. Therefore, this researcher chose the RSEI-2 model to calculate the EEQ in the study area.

### 4.2. Spatiotemporal dynamic changes

Overall, urbanization and CCD for the entire study areas both exhibited an increasing trend during 1992–2015 with growth rates of  $0.0017\text{a}^{-1}$  and  $0.0011\text{a}^{-1}$ , respectively, while the RSEI-2's change was not obvious, and its growth rate was  $1.21\text{E}^{-10}\text{a}^{-1}$  (see Fig. 4 left and Table 2). Additionally, the urbanization and CCD values both showed a strip-like distribution with a gradual decrease trend from east to west.

However, the value of RSEI-2 showed a decreasing trend from south to north. This suggested that the EEQ was better in the south and worse in the north. This is consistent with the distribution pattern of vegetation coverage in China. There are large areas of dense forests in southern China. Rich vegetation ensures the water conservation capacity of the region, inhibits the rise of surface temperature, alleviates regional water and soil loss and plays an important role in the regional ecological environment. Shandong Province and Jiangsu Province had the worst EEQ in coastal areas (Fig. 4 H). According to the data released by the China Statistics Bureau, Shandong Province and Jiangsu Province are the top two provinces of power consumptions in China. Huge energy consumption intensifies the risk of ecological environment deterioration, and these areas lack dense vegetation and efficient ecological restoration capacity. The spatial distribution differences for the three indexes exhibited the same characteristic of weakness in the west and strong in the east (Fig. 4 right). At province level, the urbanization and CCD values for most provinces fluctuated very little, and their rate of change ranged from  $0.0003\text{a}^{-1}$  to  $0.0059\text{a}^{-1}$  and  $0.0002\text{a}^{-1}$  to  $0.0186\text{a}^{-1}$ , respectively. Additionally, although the RSEI-2 value was basically unchanged with its range of  $-0.0024\text{a}^{-1}$ – $0.0013\text{a}^{-1}$ , the average value of RSEI-2 varied greatly for the various provinces, showing a distribution pattern with a small value in the northern provinces and a large value in the southern provinces (Fig. 4 left and Table 2). This indicated that the urbanization and CCD at province levels had relatively small spatial variabilities, but the CCD had relatively large spatial variabilities.

The growth area for urbanization was mainly distributed in the eastern coastal areas of China, such as the Beijing-Tianjin-Hebei urban agglomerations, the Yangtze River Delta urban agglomerations, and the Pearl River Delta urban agglomerations (the yellow area in the map in Fig. 5c). This was mainly due to the advantageous geographical location and the promotion of reform and migration policies (Du et al., 2018). Coastal cities are mostly regional central cities or administrative centers, which have attracted a large number of immigrants and investment in the recent 24 years, bringing power and resources to the urbanization. The rapid growth of economy and population, as well as the expansion of impervious surface, have led to the increase of urbanization in the region. Simultaneously, the areas with the most serious eco-environment deterioration were also concentrated in the three major urban agglomerations in China (red area in the map in Fig. 5b), particularly the Pearl River Delta urban agglomerations. This is consistent with the research results of Zheng et al. (2020b). With the rapid economic development and urban expansion, the impervious surface increasingly occupies more ecological lands on the urban scale, resulting

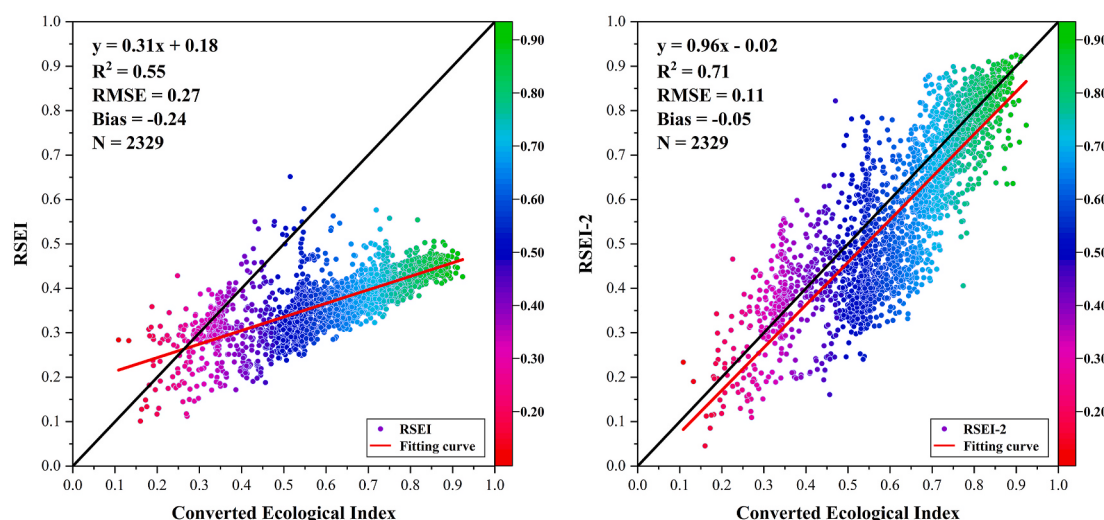


**Fig. 3.** The regional adaptation assessment results for the RSEI and the RSEI-2 using the standardized EI index.

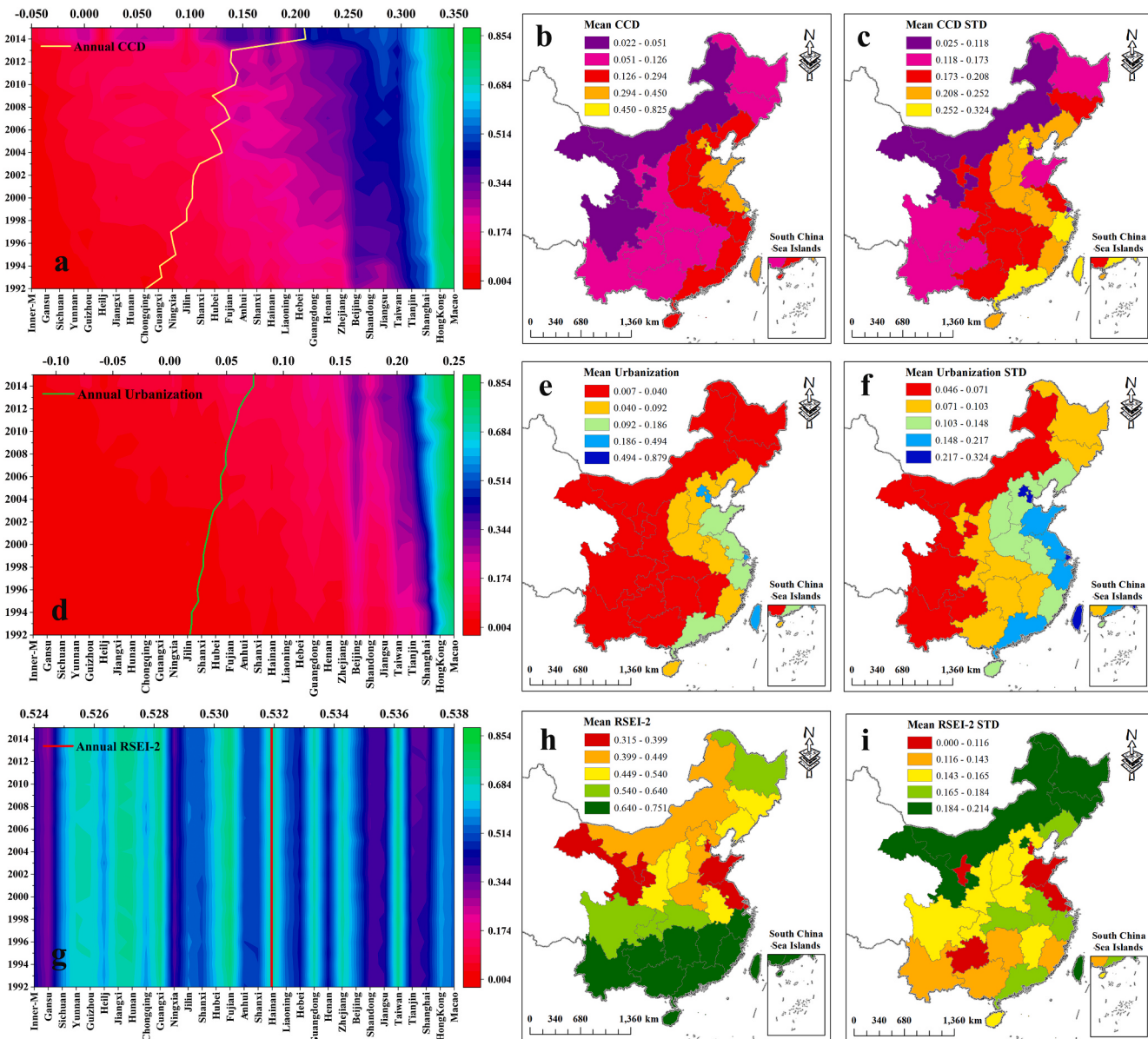


**Fig. 4.** Spatiotemporal distributions of the CCD, RSEI-2, and urbanization at provincial-scale during 1992–2015. Sub-figures (a), (d), and (g) represent the change trend of the CCD, urbanization, and the RSEI-2 for each province during 1992–2015, respectively; sub-figures (b), (e), and (h) display the spatial distributions of the CCD, urbanization, and RSEI-2 during 1992–2015, respectively; and sub-figures (c), (f), and (i) show the standard deviations' spatial distributions of the CCD, urbanization, and RSEI-2 during 1992–2015, respectively.

in the decline of vegetation coverage, which has a great impact on the EEQ. This suggested that rapid urbanization would lead to eco-environmental deterioration. Surprisingly, the CCD values for the three major urban agglomerations and their surrounding areas were still increasing (red area in the map in Fig. 5a). This indicated that deterioration of the eco-environment at this stage had no significant impact on the region's coupling coordinated development.

#### 4.3. The CCD distribution at different city levels

We divided the CCD into 9 types according to the standards in Table 3. Then, we compared cities' CCD distributions at different sizes. Additionally, according to the city scale classification standard issued by the "Notice on Adjusting the Criteria for City Size Classification" (Notice of the State Council, 2015), we divided 331 cities into five categories: megacity (MC), supercity (SC), large city (LC), medium-sized city (MSC), and petty city (PC).

**Fig. 6** shows cities' coordinating changes in central and eastern China from 1992 to 2015. Overall, the coordinated cities' spatial distributions and increases had a strong economic pattern. Specifically, the number of coordinated cities (CD) increased from 24 (7.25%) to 99 (29.91%; Fig. 6b) from 1992 to 2015. The coordinated MCs (46.67%) and SCs (42.31%) had the most significant increase, and the coordinated LCs, MSCs, and PCs also increased to a certain extent with the increasing proportions being 15.35%, 7.14%, and 13.64% (the green fold line in Fig. 6b), respectively. This implied that the coordinated cities' increases mainly existed in cities of LC size. Additionally, the MCs had the largest growth rate of the average CCD from 1992 to 2015, reaching  $39.21/10^{-4}$ a, which was twice that of PCs, followed by the SCs ( $38.87/10^{-4}$ a); the orange fold line in Fig. 6b). This indicated that the larger the city scale, the faster the degree of coupling harmony increases. In addition, as of 2015, coordinated cities were mainly distributed in MCs (11), SCs (42), and LCs (40), accounting for 73.33%, 53.85%, and 19.80%, respectively, (the magenta fold line in Fig. 6b). Among the 99

**Table 2**

The change rates ( $a^{-1}$ ) of the CCD, RSEI-2, and urbanization for each province and the entire study areas.

Province	CCD	RSEI-2	Urbanization	Province	CCD	RSEI-2	Urbanization
Beijing	0.0025	-0.0010	0.0073	Hubei	0.0011	0.0008	0.0015
Tianjin	0.0052	-0.0012	0.0124	Hunan	0.0009	0.0004	0.0012
Hebei	0.0023	0.0002	0.0033	Guangdong	0.0026	0.0002	0.0045
Shanxi	0.0014	0.0004	0.0019	Guangxi	0.0010	0.0009	0.0011
Inner Mongolia	0.0002	-0.0009	0.0003	Hainan	0.0025	0.0006	0.0029
Liaoning	0.0017	0.0000	0.0027	Chongqing	0.0013	0.0013	0.0020
Jilin	0.0008	-0.0004	0.0012	Sichuan	0.0006	0.0001	0.0008
Heilongjiang	0.0005	-0.0004	0.0007	Guizhou	0.0007	0.0009	0.0010
Shanghai	0.0059	-0.0024	0.0186	Yunnan	0.0006	0.0007	0.0008
Jiangsu	0.0057	-0.0006	0.0106	Shaanxi	0.0013	0.0009	0.0018
Zhejiang	0.0044	-0.0001	0.0074	Gansu	0.0002	-0.0003	0.0004
Anhui	0.0024	0.0009	0.0032	Ningxia	0.0011	-0.0005	0.0020
Fujian	0.0022	0.0006	0.0032	Taiwan	0.0025	0.0000	0.0050
Jiangxi	0.0010	0.0009	0.0013	Hongkong	0.0008	0.0001	0.0025
Shandong	0.0041	-0.0001	0.0061	Macao	0.0021	0.0000	0.0081
Henan	0.0030	0.0009	0.0038	Study area	0.0011	1.21E <sup>-10</sup>	0.0017

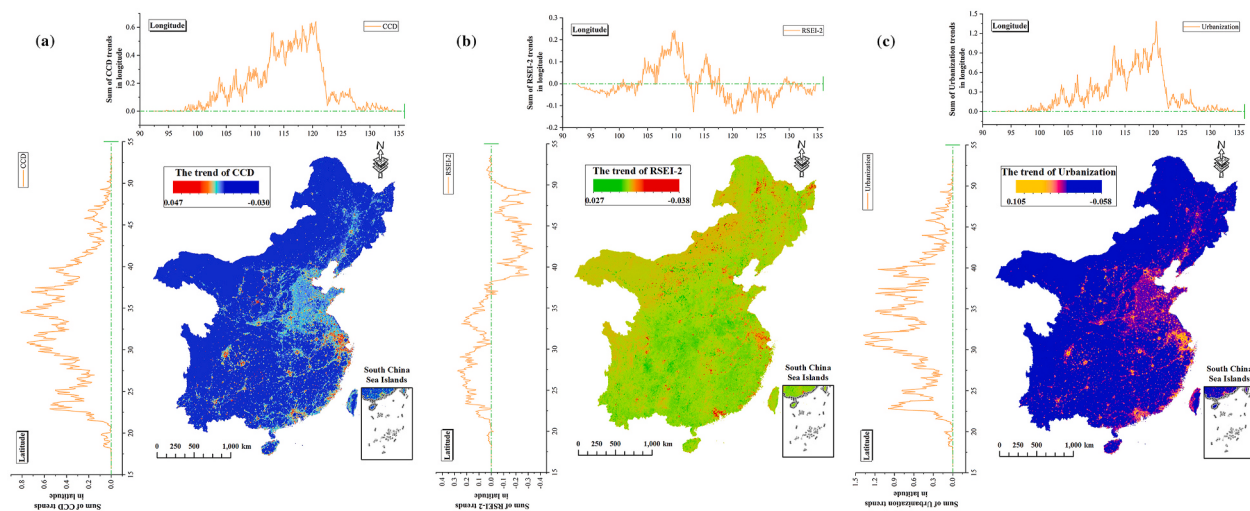


Fig. 5. Spatial distributions of the CCD's change rates (a), RSEI-2 (b), and urbanization (c) in China's central and eastern regions during 1992–2015.

**Table 3**  
Criteria for classifying CCD types.

Range of CCD	U and E	The coordination type	Flags
0 ≤ CCD < 0.15	E – U < -0.05	EI	UD. (E lags)
	E – U > 0.05	E2	UD. (U lags)
	E – U  ≤ 0.05	E3	UD. (U & E are in balance)
0.15 ≤ CCD < 0.35	E – U < -0.05	E4	MD. (E lags)
	E – U > 0.05	E5	MD. (U lags)
	E – U  ≤ 0.05	E6	MD. (U & E are in balance)
0.35 ≤ CCD < 1	E – U < -0.05	E7	CD. (E lags)
	E – U > 0.05	E8	CD. (U lags)
	E – U  ≤ 0.05	E9	CD. (U & E are in balance)

UD (Uncoordinated, UD), MD (Moderate-coordinated, MD), CD (Coordinated, CD).

coordinated cities, 16 coordinated cities were located in Shandong province, while the cities of Chengdu, Wuhan, Ezhou, and Weinan were the few coordinated cities located in the inland provinces (the blue and purple points in Fig. 6a). This suggested that the coordinated cities' spatial distributions mainly were mainly located in cities at LC size.

During 2015, only 12 out of 331 cities had lagged urbanization in terms of EEQ, including 3 MCs, 4 SCs, 3 LCs, and 2 PCs (Hong Kong and Macao), accounting for 25%, 5.71%, 1.53%, and 10.53% of their respective city size groups (the purple fold line in Fig. 6c), respectively. This suggested that EEQ outperforms urbanization for the values at

different city sizes. Additionally, urbanization growth rate for PCs was the slowest ( $24.16/10^{-4}a$ ), while that for MCs was the highest ( $88.84/10^{-4}a$ ; the orange-red fold line in Fig. 6c) during 1992–2015, and this was 3.67 times of that for SCs. This indicated that the larger the city size, the faster the urbanization rate. However, MCs exhibited the fastest deterioration of the eco-environment ( $-5.06/10^{-4}a$ ), while the EEQ growth for PCs showed the fastest trend ( $6.12/10^{-4}a$ ; the green fold line in Fig. 6c). This reflected the urbanization level and the EEQ's inconsistency direction.

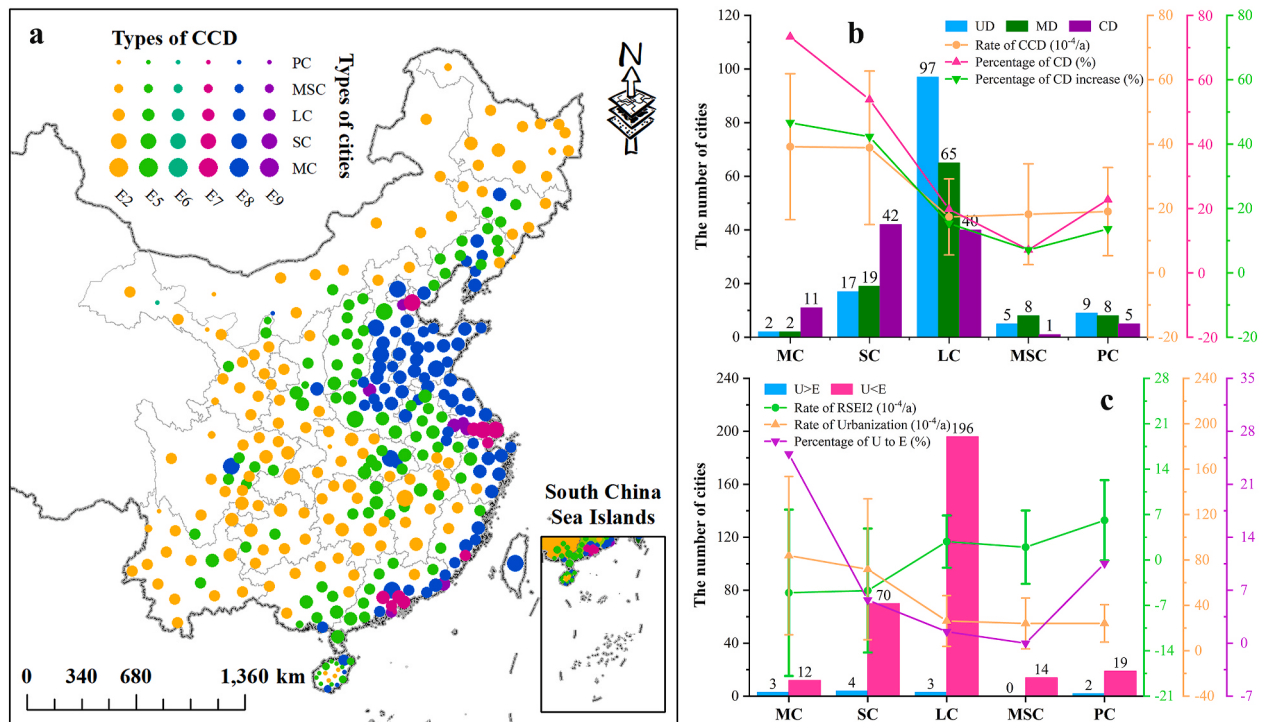


**Fig. 6.** The coupling type changes of the cities in China's central and eastern regions from 1992 to 2015: a. spatial distribution map of the cities' coupling types at the different city sizes during 2015; b. the number of different city coupling types at different city sizes during 2015 (histogram), the CCD change rates of cities at different city sizes during 1992–2015 (orange red fold line), the CD percentage at different city sizes during 2015 (magenta fold line), and the CCD increase percentage at different city sizes during 1992–2015 (green fold line); and c. the number of cities in U lags and E lags at different city sizes during 2015, the change rate of the RSEI-2 (green fold line) and urbanization (orange-red fold line) at different city sizes during 1992–2015, and the number of the U lags converted to E lags cities (magenta fold line) at different city sizes from 1992 to 2015.

#### 4.4. Spatial dependency of CCD

This study explored the CCD spatial clustering characteristics at the “city” units during 1992, 2004, and 2015 using the local autocorrelation analysis method (Ord and Getis, 2001). Fig. 7 showed that the Moran's I value for each year was higher than 0.69; the scatter points were mainly distributed in the first and third quadrants. This indicated that the CCD values' spatial distributions presented a strong agglomerations feature, i.e., the cities with high (low) CCD values were inclined to cluster. Simultaneously, the CCD distribution exhibited a pattern of “low in the West and high in the East”, that is, the LL type cities were mainly distributed in the inland China, while the HH type cities were mainly distributed in Beijing Tianjin Hebei, Yangtze River Delta, and Pearl River Delta urban agglomerations ( $P < 0.05$ , the significance distribution maps in Fig. 7).

#### 4.5. Relationships among RSEI-2, urbanization, and CCD

We ranked 331 cities in China's central and eastern regions in reverse order (see Fig. 8). Each bubble represented a city, and the size of each bubble was mapped to the CCD's change rate of each city with the lowest value of  $0a^{-1}$  and the highest value of  $0.0111a^{-1}$ . By fitting all the cities' sample points, we found that it presented a negative correlation relationship between the urbanization development and EEQ (fitting curve in the middle of Fig. 8). This indicated that urbanization development had a negative impact on the EEQ. Therefore, paying attention to the ecological environment's protection is essential for urban sustainability development in the future.

In addition, Fig. 8 draws a fold line chart of urbanization's trend ranking, the EEQ, and CCD at 331 cities. We found that the relationship between the urbanization trend ranking and CCD trend ranking presented “tortuous rise” with the fitting line's slope rate being 0.979 and

$R^2$  being 0.96. This indicated that the faster the urbanization development, the faster the CCD level, but the EEQ and CCD trend rankings both showed an abnormal negative correlation. Therefore, we speculated that urbanization development at this stage was a decisive factor affecting the CCD level, and the EEQ's excessive growth would have a negative impact on the CCD level.

## 5. Discussion

### 5.1. Analysis of coupling mechanism between urbanization and RSEI-2

Based on the analysis in Section 4.5, we speculated that: 1) at this stage, urbanization determined the CCD level-development, and the EEQ changes had little effect on the CCD level. 2) There was a linear negative relationship between urbanization and EEQ. In order to quantitatively prove the above conjecture, we evenly selected 6060 sample points from the CCD, RSEI-2 and the urbanization data in 2015. Then, we drew a three-dimensional distribution diagram of the sample points and a three-dimensional function diagram of the CCD model (Fig. 9). Finally, we characterized the urbanization and EEQ's degree of influence on the CCD using the tangent plane's slope in urbanization and the RSEI-2's two dimensions. The tangent plane was calculated as follows:

$$CCD - CCD_0 = F'_U(U - U_0) + F'_E(E - E_0) \quad (12)$$

where  $CCD$  was CCD,  $F'_U$  and  $F'_E$  were the urbanization and RSEI-2's partial derivatives, respectively, and  $CCD_0$ ,  $U_0$ , and  $E_0$  were the CCD's mean values, urbanization, and the EEQ during 2015, where their values were 0.445, 0.074, and 0.532, respectively.

As can be seen from Fig. 9 (right), the CCD's growth rate in the urbanization component is 1.505, while that in the RSEI-2 component is only 0.209, i.e., urbanization impact on the CCD is 7.2 times of the EEQ

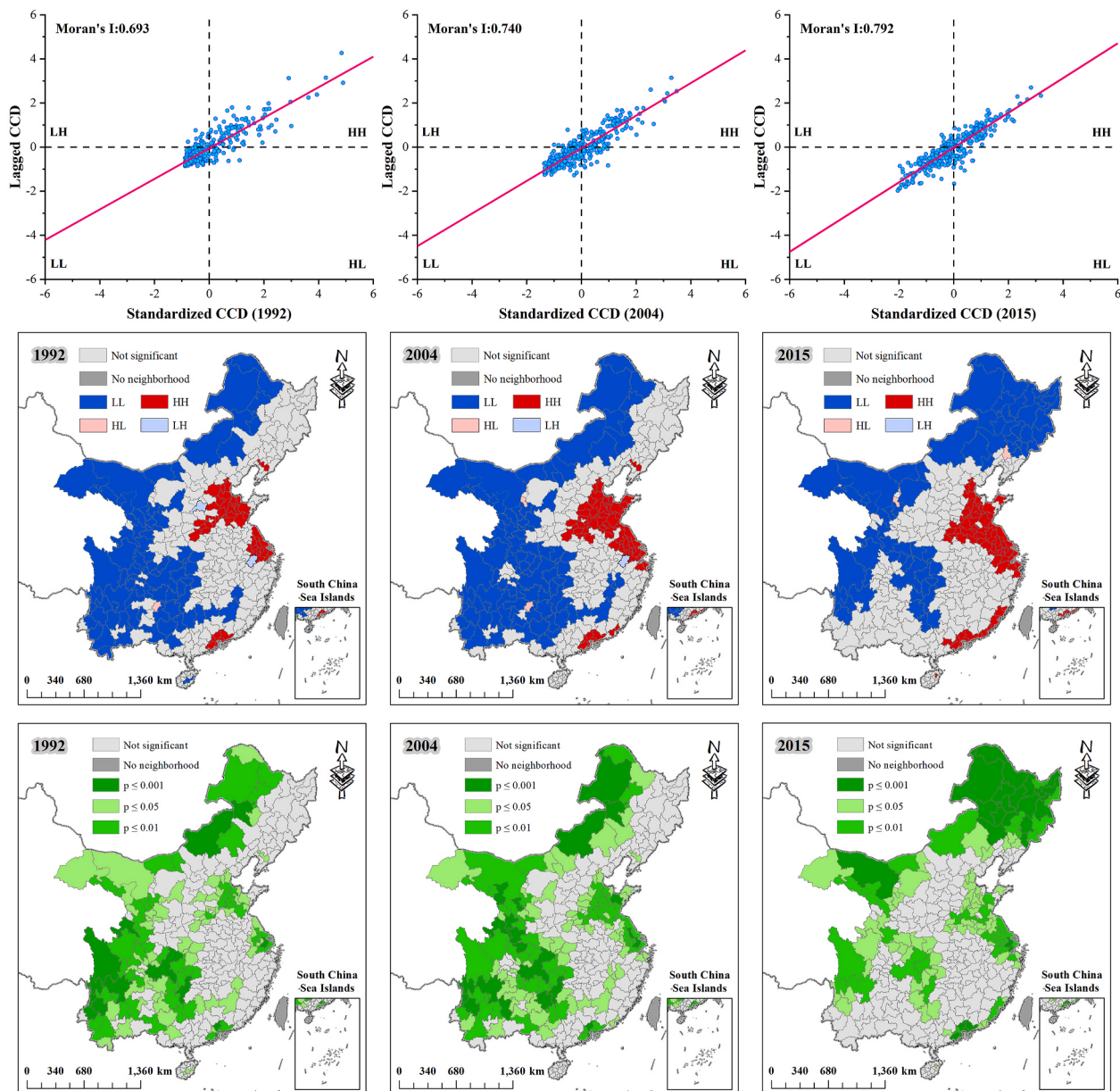


**Fig. 7.** The local Moran scatterplots (the top of the figure), local autocorrelation cluster maps (the middle of the figure), and CCD's significance (the bottom of the figure) distribution maps at the city scale during 1992, 2004, and 2015.

during 2015. This well confirmed the first conjecture above. Simultaneously, we found an important feature from Fig. 9 (left) that there was an obvious negative correlation between urbanization and the EEQ. This implies that urbanization and the RSEI-2 cannot be arbitrarily distributed in entire three-dimensional spaces. Instead, they restrict each other and are regularly distributed in space. Therefore, we calculated the RSEI-2, urbanization, and CCD data for the 29 provincial capital cities (including municipalities directly under the Central Government) and the entire study areas during 2015, and then we fitted the relationships between the EEQ and urbanization for these 30 research objects. The results show that there is a negative linear correlation between the EEQ and urbanization, confirming the second conjecture mentioned above.

The researchers posed the following question: does urbanization have a continuous, decisive, and positive impact on the CCD at a deeper level? Based on the conclusions obtained above, we derived [formulas 8, 9, and 10](#) as follows:

$$\begin{aligned}
 C &= \left\{ \frac{U \times E}{[(U+E)/2]^2} \right\}^{\frac{1}{2}} \Rightarrow C = \sqrt{\frac{U \times E}{T^2}} \Rightarrow C = \frac{\sqrt{U \times E}}{T} \\
 D &= \sqrt{C \times T} \Rightarrow D = \sqrt{\frac{\sqrt{U \times E}}{T} \times T} \Rightarrow D = \sqrt{\sqrt{U \times E}} \\
 \Rightarrow D &= \sqrt{\sqrt{U \times (-A \times U + B)}} \quad (A > 0, \quad 0 \leq U \leq 1)
 \end{aligned} \tag{13}$$

where the  $A$  term characterized the interaction strength between regional urbanization and the EEQ. The above derivation results indicated that the  $D$  and  $U$  presented a downward-opening parabolic relationship, i.e., the CCD presented a unimodal characteristic of “increasing first and then decreasing” with urbanization growth. This meant that urbanization development could not always have a positive impact on the CCD level.

[Fig. 10](#) shows the function diagrams of the relationship between urbanization and the CCD for 30 study objects. In [Fig. 10](#), the red dashed

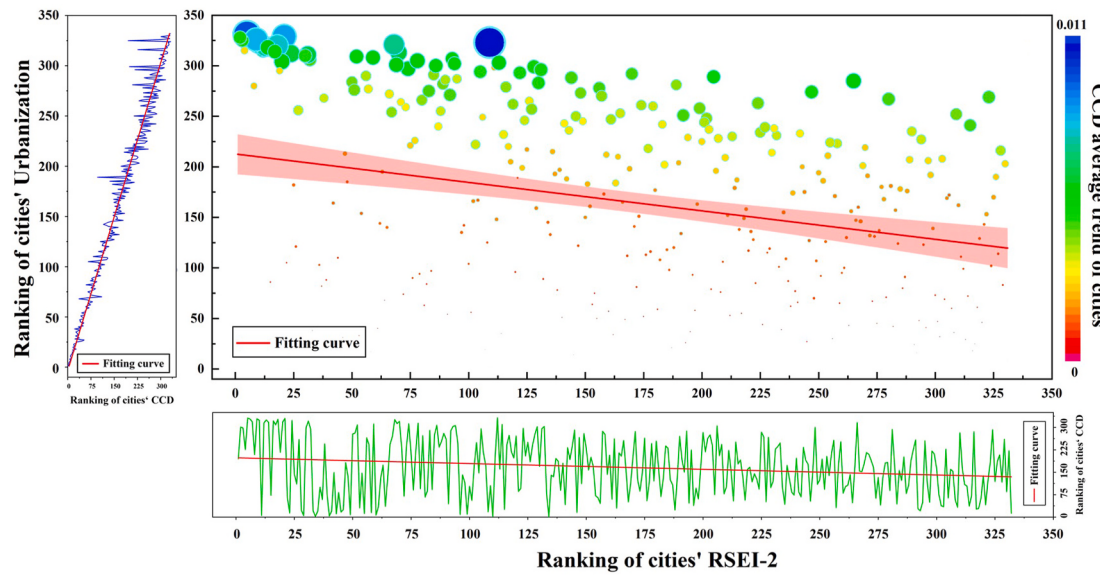


**Fig. 8.** The scatterplots between the ordered city RSEI-2 and the ordered city urbanization in central and eastern region of China during 1992–2015.

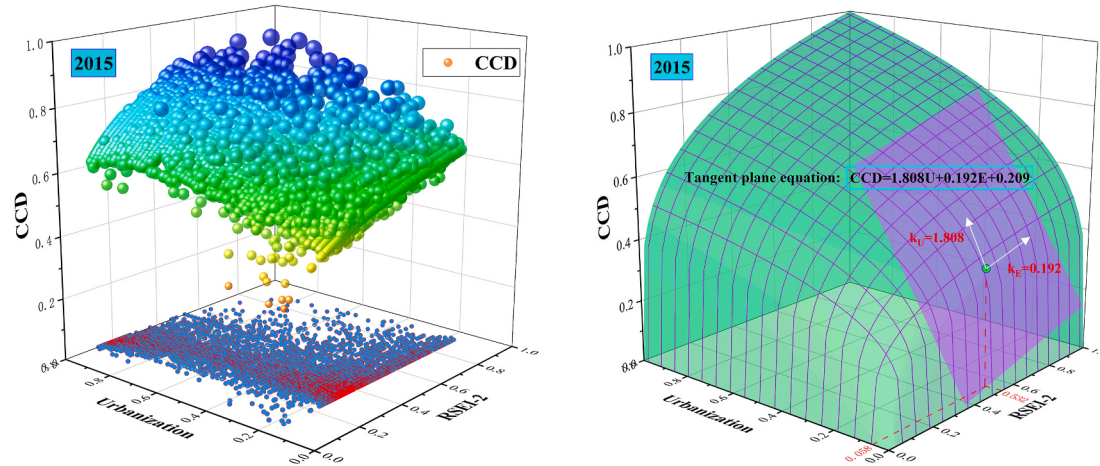


**Fig. 9.** The 3D scatter diagram for the RSEI-2, urbanization, and CCD during 2015 and the 3D function diagram of the CCD model.

line is the function's axis of symmetry, and the urbanization value corresponding to the axis of symmetry represents the turning point where the CCD value changes from an increase to a decrease under the current development status. Additionally, it can be seen from the symmetry axis's calculation formula that the symmetry axis and A show a negative correlation relationship in Eq. (13). This suggests that the symmetry axis will continue moving to the left as A increases. Therefore, the axis of symmetry can be set as a parameter representing the interaction strength between urbanization and the regional EEQ, and its numerical value controls the urbanization value interval that has a positive impact on the CCD. Additionally, Fig. 10 shows that there is a significant difference for the symmetry axis's distribution of each city. This suggests that it has a greatly different for the positive urbanization impact on the CCD at the different cities. For example, Haikou, Changchun, and Shenyang have relatively strong regulatory capabilities, while Beijing, Hangzhou, Fuzhou, and Guangzhou have relatively weak regulatory capabilities.

It is worth noting that the symmetry axis for some cities in Fig. 10 exceeds 1, and the range of U is between 0 and 1. Does this mean that these cities can arbitrarily speed the pace of urbanization development and ignore the ecological environment's protection? It should be noted that the relationship curve between urbanization and the CCD depends

on the interaction strength between the EEQ and urbanization. The A of the relationship curve should also increase, and the axis of symmetry should accordingly decrease if the ecological environment's protection is neglected in the urbanization process. When the axis of symmetry is less than 1, urbanization development will threaten the CCD level. Therefore, the ecological environment's protection cannot be ignored during the urbanization process, especially in cities whose symmetry axis is between 0 and 1.

In summary, we successfully proved the two conjectures proposed at the beginning of this section by using a rigorous method of combining mathematics and geometry. Simultaneously, we further proved that continuous urbanization development could not have a continuous positive impact on the CCD level. We hope that by exploring the coupling mechanism between the EEQ and urbanization, this study can assist scholars in implementing more in-depth research on related aspects in the future.

## 5.2. Prediction of future CCD

The CCD's future developmental direction between the EEQ and urbanization in China's central and eastern regions has important reference significance for the China 2030 Sustainable Development

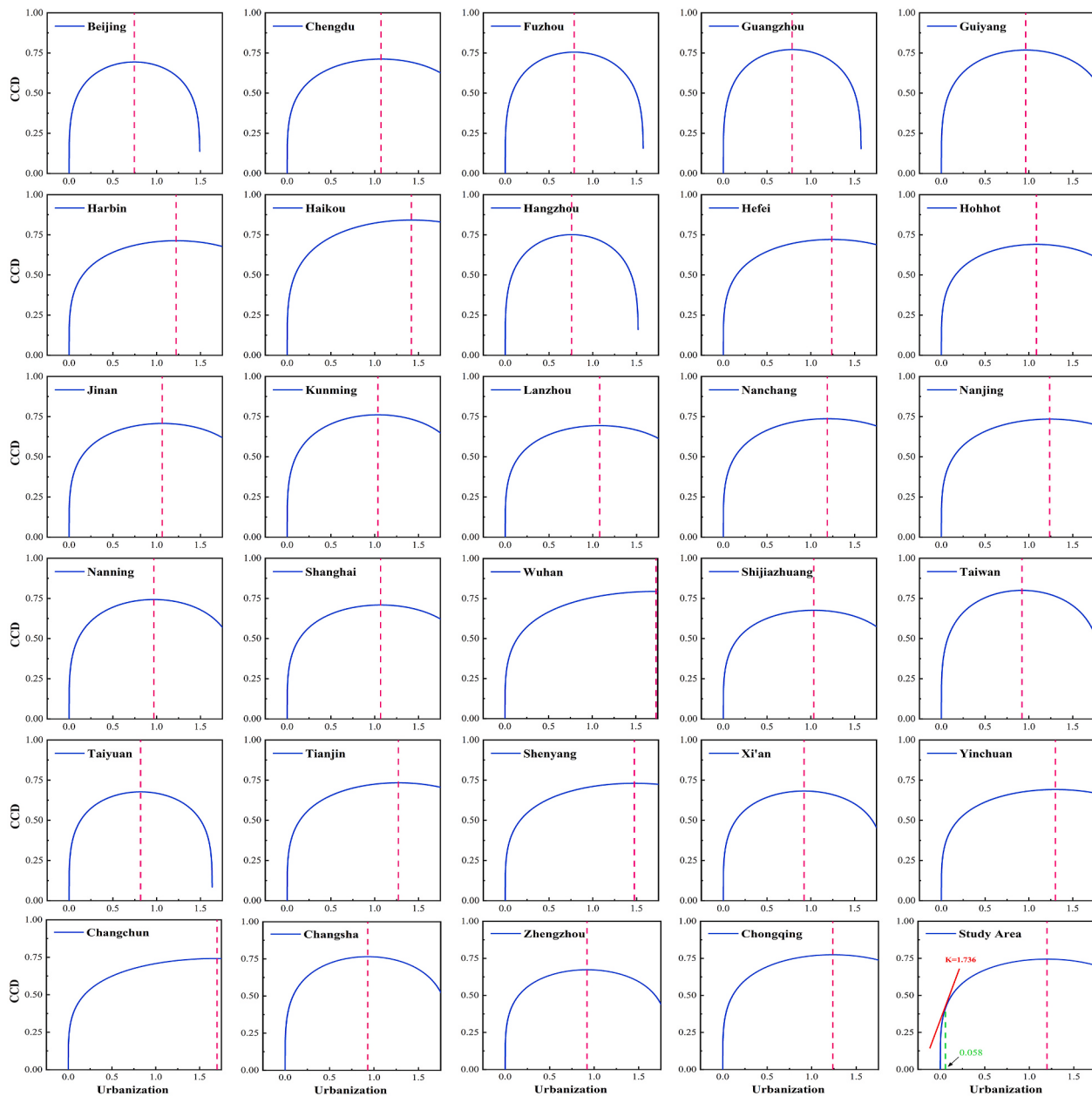


**Fig. 10.** The function diagram of the relationship between urbanization and the CCD. It should be noted that the function graph shows the relationship between CCD and urbanization in space in each city in 2015, not the relationship in time. The pink dotted line is the symmetry axis of the function curve, i.e., the turning point of the CCD from increasing to decreasing. When the axis of symmetry is located on the right side of 1, it indicates that the CCD of the region in 2015 shows a single increasing trend with the change of urbanization, because the urbanization cannot exceed 1. On the contrary, when the axis of symmetry is located on the left of 1, it indicates that there is a critical value for the positive influence of urbanization on the CCD. When the urbanization exceeds this critical value, the CCD will continue to decrease.

Goals realization. The Hurst index (Davies and Harte, 1987) has advantages in measuring self-similarity and long-term dependence of the index time series. The methods for estimating the Hurst index include R/S analysis, wavelet analysis, whittle method, residual variance method, absolute value method, and aggregate variance periodogram method (Bhattacharya et al., 1983; Carbone et al., 2004). Thus, this study predicts the CCD's future changes in central and eastern regions of China based on the CCD's change trend during 1992–2015 using R/S analysis method.

It can be seen from Fig. 11 that the regions with significant long-term CCD dependence are mainly distributed in China's three major urban agglomerations and Taiwan. Additionally, the change types are mainly red and blue. This indicated that the CCD in most areas increased in the

past, and this is consistent with the results in Section 4.2. The four regions all show large areas of CCD reduction in the future (blue and cyan), particularly in the Beijing-Tianjin-Hebei urban agglomerations, the inner Pearl River Delta urban agglomerations, northern Jiangsu, and the three cities of Taipei, Tainan, and Taichung.

Fig. 12 shows that the area, the area percentage and the cumulative frequency of different Hurst values of Beijing-Tianjin-Hebei Province, the Pearl River Delta, the Yangtze River Delta urban agglomerations and Taiwan. It can be seen from Fig. 12 that in terms of the development trend, most areas in the Pearl River Delta, the Yangtze River Delta urban agglomerations and Taiwan showed an increasing trend in the CCD, and UU types played a dominant role. Among them, Taiwan exhibited the highest increase in the CCD area (61.85%), followed by the Yangtze

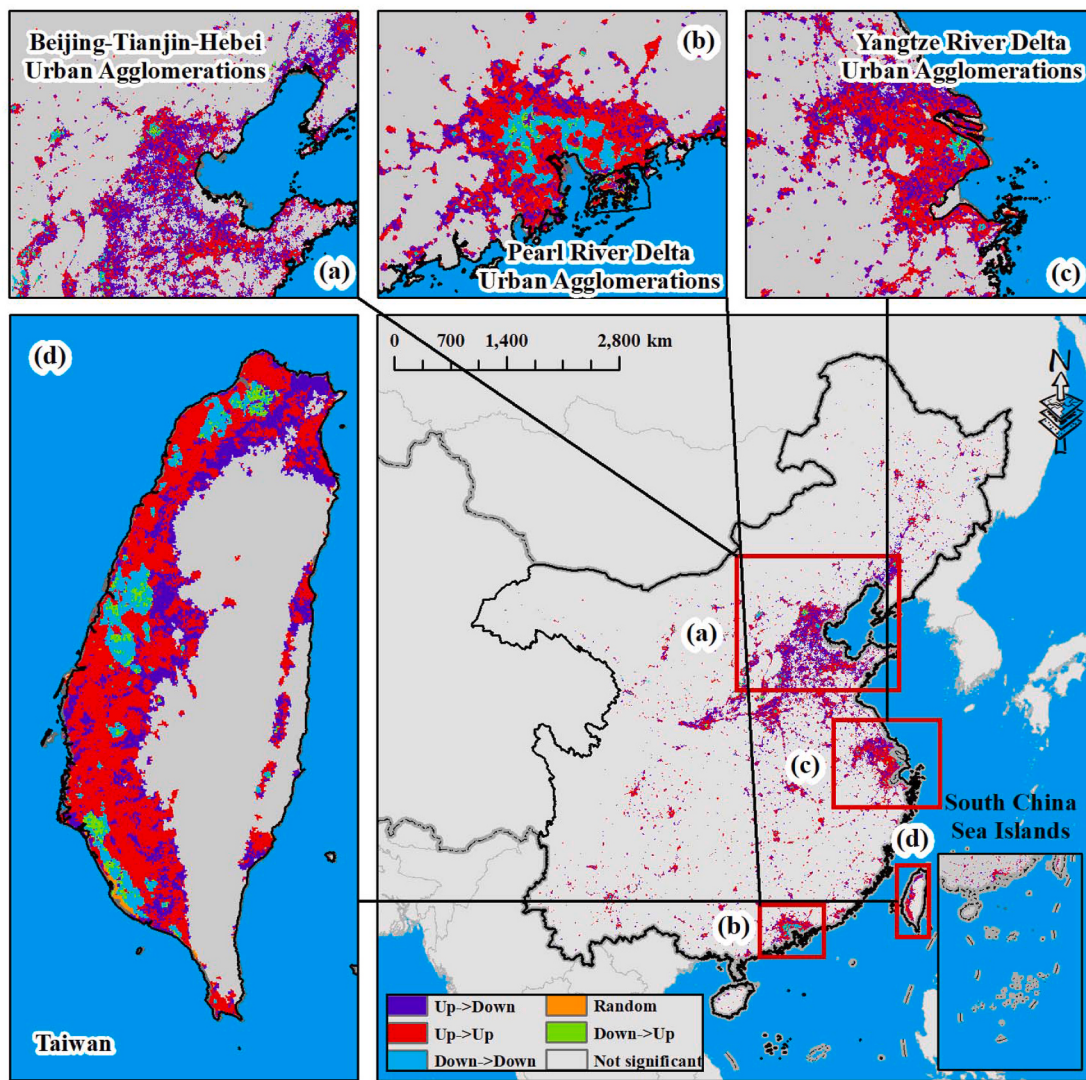


Fig. 11. The spatial distribution map of the CCD using the Hurst exponent.

River Delta urban agglomerations (56.29%) and the Pearl River Delta urban agglomerations (56.26%). On the contrary, Beijing-Tianjin-Hebei Province urban agglomerations showed a large decrease in the CCD area, with an area of  $71.59 \times 10^3 \text{ km}^2$  in the future. It indicates that the momentum of growth in Beijing, Tianjin and Hebei Province was insufficient and that the urbanization development was stagnating or even declining. Among these four regions, the Yangtze River Delta urban agglomerations showed the largest increase in the CCD area reaching  $60.35 \times 10^3 \text{ km}^2$ , whilst Taiwan had the smallest area ( $14.109 \times 10^3 \text{ km}^2$ ). The Yangtze River Delta urban agglomeration had the highest percentage of area increase in CCD in the past, with a rate of 94.79%, while the Pearl River Delta showed the smallest increase (81.225%), followed by Taiwan (86.364%).

Therefore, we propose the following suggestions: (1) strategies pertaining to Beijing-Tianjin-Hebei urban agglomerations and the Pearl River Delta urban agglomerations, where the EEQ is currently showing a downward trend, should focus on green economy development, the acceleration of technological transformation and innovation, and the formulation of sound environmental protection policies. (2) Strategies pertaining to the northern Jiangsu should be used to increase the tertiary industry's proportion, introduce foreign investment, continuously improve infrastructure construction, and steadily increase urbanization level, while also focusing on ecological environment protection; (3) the urbanization development of Taiwan Province, affected by the

international situation, has continued to decline in the past 24 years, and thus, Taiwan should accelerate economic transformation, increase investment preferences, actively introduce foreign capital, promote independent brand building, increase exports, improve infrastructure construction, and improve relations with mainland China.

## 6. Conclusion

China's rapid urbanization process has produced serious ecological and environmental problems since the establishment of the socialist market economic system during 1992–2015. Simultaneously, “sustainable development” has become a global strategic development goal, so the country needs to properly and quickly achieve the China 2030 Sustainable Development Goals. Therefore, the researchers of this study monitored the spatiotemporal changes of the EEQ, urbanization, and the CCD in the central and eastern regions of China during 1992–2015 and then quantitatively studied the coupling mechanism between the EEQ and urbanization using the CCD model based on multi-source remote sensing data. This study will counterbalance deficiencies of the existing research, fill gaps in the current research on the interaction mechanism between the EEQ and urbanization, and provide a new research perspective for understanding urban sustainable development in China and even the world. Key points from the conclusion are as follows:

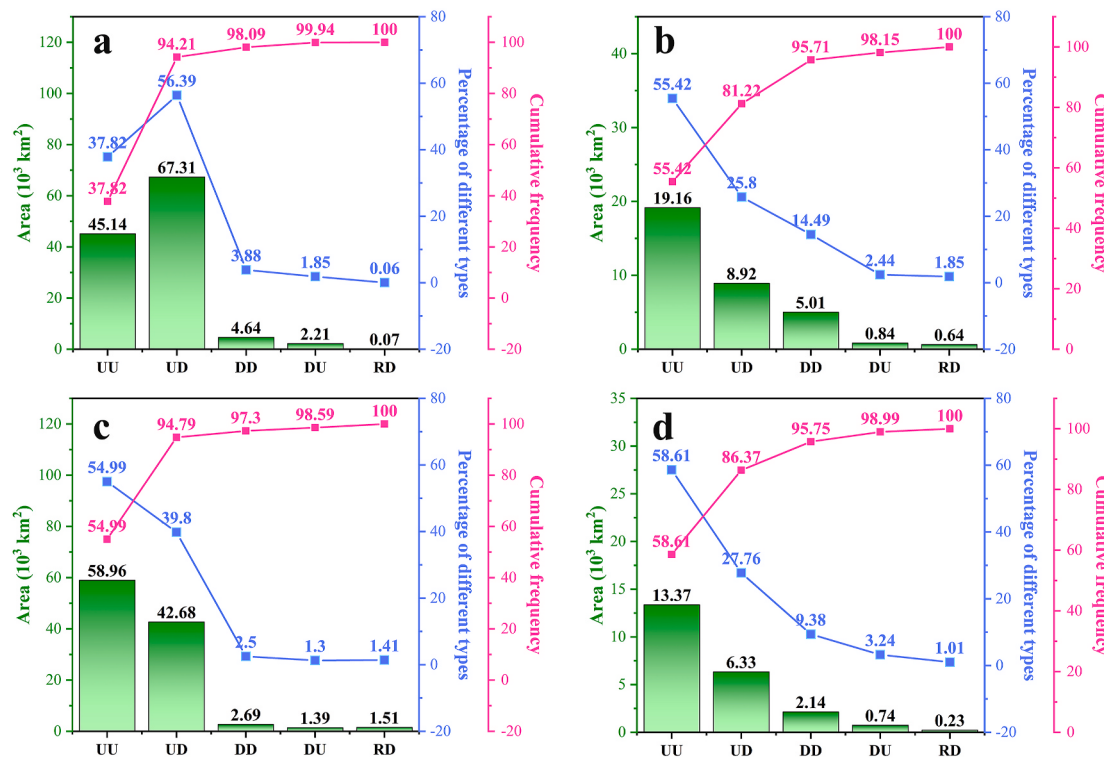


**Fig. 12.** The area (green column), area percentage and cumulative frequency (blue broken line) of different Hurst values in (a) Beijing-Tianjin-Hebei Province, (b) Pearl River Delta, (c) Yangtze River Delta urban agglomerations and (d) Taiwan. UU, UD, DD, DU and RD represent from Up to Up, from Up to Down, from Down to Down, from Down to Up and random changes, respectively.

- (1) During 1992–2015, the urbanization and CCD values for the entire study area exhibited an increasing trend with the growth rates being  $0.0017\text{a}^{-1}$  and  $0.0011\text{a}^{-1}$ , respectively, while the RSEI-2 showed slight change, and its growth rate was  $1.21 \times 10^{-10} \text{a}^{-1}$ . Spatially, urbanization and the CCD both presented a gradual decrease from east to west, while the RSEI-2 displayed a gradual decrease from south to north, exhibiting a “good in the south and bad in the north” spatial distributions. Additionally, the violent spatial variability for the three indexes all exhibited the spatial distribution patterns of weak in the west and strong in the east. For the CCD, its changes in the central and eastern regions of China had strong spatial agglomerations, especially in the three major China’s urban agglomerations. Additionally, the CCD had a strong spatial dependence, i.e., the cities with high (low) CCD values were more likely to cluster, exhibiting a spatial pattern of “low inside, high outside, high in the east, low in the west”.
- (2) There was a negative linear relationship (i.e., a “unimodal” functional relationship) between the EEQ and urbanization. Additionally, urbanization development had a decisive influence on the CCD in the past 24 years due to the huge gap between the two indexes development levels. However, the continuous “rough” urbanization process could not have a sustained positive impact on the CCD level between urbanization and the EEQ, i.e., there was a critical value of positive impact. For example, the future CCD level between EEQ and urbanization would decline in three major urban agglomerations and Taiwan.
- (3) By dividing the CCD into three types (i.e., uncoordinated, moderate-coordinated, and coordinated), the coordinated city types were mainly distributed in MCs, SCs, and LCs, i.e., the higher the city’s level of economic development, the better the cities’ coordination, but the cities’ EEQ continued to deteriorate.
- (4) The RSEI-2 model proposed in this study is suitable for monitoring the EEQ at the national and regional scales. The RSEI-2 model has the advantages of simplicity, convenience, and data

accessibility, and thus, provides the second choice after EI index for monitoring China’s EEQ.

#### CRediT authorship contribution statement

**Dong Xu:** substantially contributed to the data gathering and analysis and paper writing. **Feng Yang:** substantially contributed to conceptualization and paper editing and revising. **Le Yu:** substantially contributed to conceptualization and paper editing and revising. **Yuyu Zhou:** substantially contributed to the design of the study methods. **Haixing Li:** substantially contributed to the design of the study methods. **Jinji Ma:** substantially contributed to the programming. **Jincui Huang:** substantially contributed to the programming. **Jing Wei:** substantially contributed to the reviewing. **Yang Xu:** substantially contributed to the reviewing. **Chong Zhang:** substantially contributed to the reviewing. **Jie Cheng:** substantially contributed to the reviewing.

#### Declaration of competing interest

The authors declare that they have no known competing financial interests or personal relationships that could have appeared to influence the work reported in this paper.

#### Acknowledgements

This work was partly supported by the National Natural Science Foundation of China via grant 41771365, the National Key Research and Development Program of China via grant 2016YFA0600101 and the National Natural Science Foundation of China via grant 41371323. Thanks to the Ministry of Ecology and Environment of the People’s Republic of China for providing the National County eco-environmental index data, which played an important role in our research. The authors thank AiMi Academic Services ([www.aimieditor.com](http://www.aimieditor.com)) for English language editing and review services.

## References

- HJ 192-2015, Technical Criterion for Ecosystem Status Evaluation[S].
- Abu Hammad, A., Tumeizi, A., 2012. Land degradation: socioeconomic and environmental causes and consequences in the eastern Mediterranean. *Land Degrad. Dev.* 23 (3), 216–226. <https://doi.org/10.1002/ldr.1069>.
- Bai, Y., Wong, C.P., Jiang, B., et al., 2018. Developing China's Ecological Redline Policy using ecosystem services assessments for land use planning. *Nat. Commun.* 9 (1), 1–13. <https://doi.org/10.1038/s41467-018-05306-1>.
- Beloin-Saint-Pierre, Didier, et al., 2017. A review of urban metabolism studies to identify key methodological choices for future harmonization and implementation. *J. Clean. Prod.* 163, S223–S240. <https://doi.org/10.1016/j.jclepro.2016.09.014>.
- Bhattacharya, Rabindra N., Gupta, Vijay K., Waymire, Ed, 1983. The Hurst effect under trends. *J. Appl. Probab.* 649–662. <https://doi.org/10.1017/S00219000200023895>.
- Cai, J., Li, X., Liu, L., et al., 2021. Coupling and coordinated development of new urbanization and agro-ecological environment in China. *Sci. Total Environ.* 776. <https://doi.org/10.1016/j.scitotenv.2021.145837>, 145837.
- Capps, K.A., Bentzen, C.N., Ramírez, A., 2016. Poverty, urbanization, and environmental degradation: urban streams in the developing world. *Freshw. Sci.* 35 (1), 429–435. <https://doi.org/10.1086/684945>.
- Carbone, Anna, Castelli, Giuliano, Eugene Stanley, H., 2004. Time-dependent Hurst exponent in financial time series. *Phys. Stat. Mech. Appl.* 344 (1–2), 267–271. <https://doi.org/10.1016/j.physa.2004.06.130>.
- Chen, J., Zhuo, L., Shi, P.J., et al., 2003. The study on urbanization process in China based on DMSP/OLS data: development of a light index for urbanization level estimation. *JOURNAL OF REMOTE SENSING-BEIJING-* 7 (3), 168–175.
- Chen, Jiandong, et al., 2020. Coupling coordination between carbon emissions and the eco-environment in China. *J. Clean. Prod.* 276, 123848. <https://doi.org/10.1016/j.jclepro.2020.123848>.
- Chikaraishi, M., Fujiwara, A., Kaneko, S., et al., 2015. The moderating effects of urbanization on carbon dioxide emissions: a latent class modeling approach. *Technol. Forecast. Soc. Change* 90, 302–317. <https://doi.org/10.1016/j.techfore.2013.12.025>.
- Crist, E.P., 1985. A TM tasseled cap equivalent transformation for reflectance factor data. *Rem. Sens. Environ.* 17 (3), 301–306. [https://doi.org/10.1016/0034-4257\(85\)90102-6](https://doi.org/10.1016/0034-4257(85)90102-6).
- Cui, D., Chen, X., Xue, Y., et al., 2019. An integrated approach to investigate the relationship of coupling coordination between social economy and water environment on urban scale-A case study of Kunming. *J. Environ. Manag.* 234, 189–199. <https://doi.org/10.1016/j.jenvman.2018.12.091>.
- Davies, Robert B., Harte, D.S., 1987. Tests for Hurst effect. *Biometrika* 74 (1), 95–101. <https://doi.org/10.1093/biomet/74.1.95>.
- Dou, Y., Kuang, W., 2020. A comparative analysis of urban impervious surface and green space and their dynamics among 318 different size cities in China in the past 25 years. *Sci. Total Environ.* 706, 135828. <https://doi.org/10.1016/j.scitotenv.2019.135828>.
- Du, Y., Sun, T., Peng, J., et al., 2018. Direct and spillover effects of urbanization on PM2.5 concentrations in China's top three urban agglomerations. *J. Clean. Prod.* 190, 72–83. <https://doi.org/10.1016/j.jclepro.2018.03.290>.
- Ermidia, Sofía L., et al., 2020. Google earth engine open-source code for land surface temperature estimation from the Landsat series. *Rem. Sens.* 12 (9), 1471. <https://doi.org/10.3390/rs12091471>.
- Fan, Y., Fang, C., Zhang, Q., 2019. Coupling coordinated development between social economy and ecological environment in Chinese provincial capital cities-assessment and policy implications. *J. Clean. Prod.* 229, 289–298. <https://doi.org/10.1016/j.jclepro.2019.05.027>.
- Fan, W., Wang, H., Liu, Y., et al., 2020. Spatio-temporal variation of the coupling relationship between urbanization and air quality: a case study of Shandong Province. *J. Clean. Prod.* 272, 122812. <https://doi.org/10.1016/j.jclepro.2020.122812>.
- Fang, ChuangLin, Ren, YuFei, 2017. Analysis of emergy-based metabolic efficiency and environmental pressure on the local coupling and telecoupling between urbanization and the eco-environment in the Beijing-Tianjin-Hebei urban agglomeration. *Sci. China Earth Sci.* 60 (6), 1083–1097. <https://doi.org/10.1007/s11430-016-9038-6>.
- Fang, Chuanglin, Wang, Jing, 2013. A theoretical analysis of interactive coercing effects between urbanization and eco-environment. *Chin. Geogr. Sci.* 23 (2), 147–162. <https://doi.org/10.1007/s11769-013-0602-2>.
- Fang, Chuanglin, Wang, Shaojian, Li, Guangdong, 2015. Changing urban forms and carbon dioxide emissions in China: a case study of 30 provincial capital cities. *Appl. Energy* 158, 519–531. <https://doi.org/10.1016/j.apenergy.2015.08.095>.
- Fang, Chuanglin, Liu, Haimeng, Li, Guangdong, 2016. International progress and evaluation on interactive coupling effects between urbanization and the eco-environment. *J. Geogr. Sci.* 26 (8), 1081–1116. <https://doi.org/10.1007/s11442-016-1317-9>.
- Fang, C., Zhou, C., Gu, C., et al., 2017. A proposal for the theoretical analysis of the interactive coupled effects between urbanization and the eco-environment in mega-urban agglomerations. *J. Geogr. Sci.* 27 (12), 1431–1449. <https://doi.org/10.1007/s11442-017-1445-x>.
- Fang, C., Cui, X., Li, G., et al., 2019. Modeling regional sustainable development scenarios using the Urbanization and Eco-environment Coupler: case study of Beijing-Tianjin-Hebei urban agglomeration, China. *Sci. Total Environ.* 689, 820–830. <https://doi.org/10.1016/j.scitotenv.2019.06.430>.
- Fanning, Andrew L., Daniel, W., O'Neill, Büchs, Milena, 2020. Provisioning systems for a good life within planetary boundaries. *Global Environ. Change* 64, 102135. <https://doi.org/10.1016/j.gloenvcha.2020.102135>.
- Feng, Y., He, S., Li, G., 2021. Interaction between urbanization and the eco-environment in the Pan-Third Pole region. *Sci. Total Environ.* 148011. <https://doi.org/10.1016/j.scitotenv.2021.148011>.
- Fu, S., Zhuo, H., Song, H., et al., 2020. Examination of a coupling coordination relationship between urbanization and the eco-environment: a case study in Qingdao, China. *Environ. Sci. Pollut. Control Ser.* 27 (19), 23981–23993. <https://doi.org/10.1007/s11356-020-08683-7>.
- Geng, Y., Zhang, H., 2020. Coordination assessment of environment and urbanization: hunan case. *Environ. Monit. Assess.* 192 (10), 1–18. <https://doi.org/10.1007/s10661-020-08598-3>.
- Gorelick, Noel, et al., 2017. Google earth engine: planetary-scale geospatial analysis for everyone. *Rem. Sens. Environ.* 202, 18–27. <https://doi.org/10.1016/j.rse.2017.06.031>.
- Grilo, F., Pinho, P., Aleixo, C., et al., 2020. Using green to cool the grey: modelling the cooling effect of green spaces with a high spatial resolution. *Sci. Total Environ.* 724, 13812. <https://doi.org/10.1016/j.scitotenv.2020.13812>.
- Gu, C., Hu, L., Zhang, X., et al., 2011. Climate change and urbanization in the Yangtze River Delta. *Habitat Int.* 35 (4), 544–552. <https://doi.org/10.1016/j.habitatint.2011.03.002>.
- Guo, B., Fang, Y., Jin, X., 2020. Monitoring the effects of land consolidation on the ecological environmental quality based on remote sensing: a case study of Chaohu Lake Basin, China. *Land Use Pol.* 95, 104569. <https://doi.org/10.1016/j.landusepol.2020.104569>.
- He, J., Wang, S., Liu, Y., et al., 2017. Examining the relationship between urbanization and the eco-environment using a coupling analysis: case study of Shanghai, China. *Ecol. Indicat.* 77, 185–193. <https://doi.org/10.1016/j.ecolind.2017.01.017>.
- Henderson, Vernon, 2003. The urbanization process and economic growth: the so-what question. *J. Econ. Growth* 8 (1), 47–71. <https://doi.org/10.1023/A:1022860800744>.
- Jalil, Z.A., Naji, H.I., Mahmood, M.S., 2020. Developing sustainable alternatives from destroyed buildings waste for reconstruction projects. *Civil Engineering Journal* 6 (1), 60–68. <https://doi.org/10.28991/cej-2020-03091453>.
- Kong, F., Yin, H., James, P., et al., 2014. Effects of spatial pattern of greenspace on urban cooling in a large metropolitan area of eastern China. *Landscape. Urban Plann.* 128, 35–47. <https://doi.org/10.1016/j.landurbplan.2014.04.018>.
- Li, X., Zhou, Y., Zhao, M., et al., 2020. A harmonized global nighttime light dataset 1992–2018. *Scientific Data* 7 (1), 1–9. <https://doi.org/10.1038/s41597-020-0510-y>.
- Liang, L., Wang, Z., Li, J., 2019. The effect of urbanization on environmental pollution in rapidly developing urban agglomerations. *J. Clean. Prod.* 237, 117649. <https://doi.org/10.1016/j.jclepro.2019.117649>.
- Liao, W., Jiang, W., 2020. Evaluation of the spatiotemporal variations in the eco-environmental quality in China based on the remote sensing ecological index. *Rem. Sens.* 12 (15), 2462. <https://doi.org/10.3390/rs12152462>.
- Li, Zhuo, Shi, Peijun, Jin, Chen, 2003. Application of compound night light index derived from DMSP/OLS data to urbanization analysis in China in the 1990s. *Acta Geograph. Sin.* 58 (6), 893–902. <https://doi.org/10.3321/j.issn:0375-5444.2003.06.013>.
- Liu, N., Liu, C., Xia, Y., et al., 2018a. Examining the coordination between urbanization and eco-environment using coupling and spatial analyses: a case study in China. *Ecol. Indicat.* 93, 1163–1175. <https://doi.org/10.1016/j.ecolind.2018.06.013>.
- Liu, N., Nana, et al., 2018b. Examining the coordination between urbanization and eco-environment using coupling and spatial analyses: a case study in China. *Ecol. Indicat.* 93, 1163–1175. <https://doi.org/10.1016/j.ecolind.2018.06.013>.
- Liu, K., Qiao, Y., Shi, T., et al., 2021. Study on coupling coordination and spatiotemporal heterogeneity between economic development and ecological environment of cities along the Yellow River Basin. *Environ. Sci. Pollut. Control Ser.* 28 (6), 6898–6912. <https://doi.org/10.1007/s11356-020-11051-0>.
- Lu, Youjin, Kong, L., Yan, Li, 2019. Measurement on the coordination degree of China's urbanization and ecological environment. *urban issues* 12, 3. <https://doi.org/10.13239/j.bjsshkxy.cswt.191202>.
- Mafi Gholami, D., Baharlouei, M., 2019. Monitoring long-term mangrove shoreline changes along the northern coasts of the Persian Gulf and the Oman Sea. *Emerging Science Journal* 3 (2). <https://doi.org/10.28991/esj-2019-01172>.
- Mao, D., Wang, Z., Wu, J., et al., 2018. China's wetlands loss to urban expansion. *Land Degrad. Dev.* 29 (8), 2644–2657. <https://doi.org/10.1002/lde.2939>.
- Martínez-Zarzoso, I., Maruotti, A., 2011. The impact of urbanization on CO<sub>2</sub> emissions: evidence from developing countries. *Ecol. Econ.* 70 (7), 1344–1353. <https://doi.org/10.1016/j.ecolecon.2011.02.009>.
- McKinney, M.L., 2008. Effects of urbanization on species richness: a review of plants and animals. *Urban Ecosyst.* 11 (2), 161–176. <https://doi.org/10.1007/s11252-007-0045-4>.
- National Earth System Science Data Center, National Science & Technology Infrastructure of China (<http://www.geodata.cn>) .
- Notice of the state council on adjusting the standards for city size classification. *Bulletin of the People's Government of Shaanxi Province* (2), 2015, 9.
- Oo, H.T., Zin, W.W., Kyi, C.C.T., 2020. Analysis of streamflow response to changing climate conditions using SWAT model. *Civil Engineering Journal* 6 (2), 194–209. <https://doi.org/10.28991/cej-2020-03091464>.
- Ord, J.K., Getis, A., 2001. Testing for local spatial autocorrelation in the presence of global autocorrelation. *J. Reg. Sci.* 41 (3), 411–432. <https://doi.org/10.1111/0022-4146.00224>.
- Rikimaru, A., Roy, P.S., Miyatake, S., 2002. Tropical forest cover density mapping. *Trop. Ecol.* 43 (1), 39–47.
- Seto, Karen C., Sánchez-Rodríguez, Roberto, Fragkias, Michail, 2010. The new geography of contemporary urbanization and the environment. *Annu. Rev. Environ. Resour.* 35. <https://doi.org/10.1146/annurev-environ-100809-125336>.

- Shan, W., Jin, X., Ren, J., et al., 2019. Ecological environment quality assessment based on remote sensing data for land consolidation. *J. Clean. Prod.* 239, 118126. <https://doi.org/10.1016/j.jclepro.2019.118126>.
- Shao, Z., Ding, L., Li, D., et al., 2020. Exploring the relationship between urbanization and ecological environment using remote sensing images and statistical data: a case study in the Yangtze River Delta, China. *Sustainability* 12 (14), 5620. <https://doi.org/10.3390/su12145620>.
- Song, Qijiao, et al., 2018. Investigation of a “coupling model” of coordination between low-carbon development and urbanization in China. *Energy Pol.* 121, 346–354. <https://doi.org/10.1016/j.enpol.2018.05.037>.
- Tian, F., Fenholz, R., Verbesselt, J., et al., 2015. Evaluating temporal consistency of long-term global NDVI datasets for trend analysis. *Rem. Sens. Environ.* 163, 326–340. <https://doi.org/10.1016/j.rse.2015.03.031>.
- Tucker, C.J., 1979. Red and photographic infrared linear combinations for monitoring vegetation. *Rem. Sens. Environ.* 8 (2), 127–150.
- Wang, Z., Deng, X., Song, W., et al., 2017a. What is the main cause of grassland degradation? A case study of grassland ecosystem service in the middle-south Inner Mongolia. *Catena* 150, 100–107. <https://doi.org/10.1016/j.catena.2016.11.014>.
- Wang, J., Sheng, Y., Wada, Y., 2017b. Little impact of the Three Gorges Dam on recent decadal lake decline across China's Yangtze Plain. *Water Resour. Res.* 53 (5), 3854–3877. <https://doi.org/10.1002/2016WR019817>.
- Xu, H., 2013a. A remote sensing index for assessment of regional ecological changes. *China Environ. Sci.* 33 (5), 889–897.
- Xu, H.Q., 2013b. A remote sensing urban ecological index and its application. *Acta Ecol. Sin.* 33 (24), 7853–7862. <https://doi.org/10.5846/stxb201208301223>.
- Xu, Y., Yu, L., Peng, D., et al., 2020. Annual 30-m land use/land cover maps of China for 1980–2015 from the integration of AVHRR, MODIS and Landsat data using the BFEST algorithm. *Sci. China Earth Sci.* <https://doi.org/10.1007/s11430-019-9606-4>.
- Yan, G., Liu, G., Marco, C., et al., 2018. Economy-pollution nexus model of cities at river basin scale based on multi-agent simulation: a conceptual framework. *Ecol. Model.* 379, 22–38. <https://doi.org/10.1016/j.ecolmodel.2018.04.004>.
- Yang, Yi, Meng, Guanfei, 2019. A bibliometric analysis of comparative research on the evolution of international and Chinese ecological footprint research hotspots and frontiers since 2000. *Ecol. Indicat.* 102, 650–665. <https://doi.org/10.1016/j.ecolind.2019.03.031>.
- Yang, Shangguang, Dong, Cao, Lo, Kevin, 2018. Analyzing and optimizing the impact of economic restructuring on Shanghai's carbon emissions using STIRPAT and NSGA-II. *Sustainable cities and society* 40, 44–53. <https://doi.org/10.1016/j.scs.2018.03.030>.
- Yu, Z., Qin, T., Yan, D., et al., 2018. The impact on the ecosystem services value of the ecological shelter zone reconstruction in the upper reaches basin of the Yangtze River in China. *Int. J. Environ. Res. Publ. Health* 15 (10), 2273. <https://doi.org/10.3390/ijerph15102273>.
- Zhang, Zhengxian, Li, Yun, 2020. Coupling coordination and spatiotemporal dynamic evolution between urbanization and geological hazards—A case study from China. *Sci. Total Environ.* 138825. <https://doi.org/10.1016/j.scitotenv.2020.138825>.
- Zhao, Y., Wang, S., Zhou, C., 2016. Understanding the relation between urbanization and the eco-environment in China's Yangtze River Delta using an improved EKC model and coupling analysis. *Sci. Total Environ.* 571, 862–875. <https://doi.org/10.1016/j.scitotenv.2016.07.067>.
- Zheng, Z., Wu, Z., Chen, Y., et al., 2020a. Exploration of eco-environment and urbanization changes in coastal zones: a case study in China over the past 20 years. *Ecol. Indicat.* 119, 106847. <https://doi.org/10.1016/j.ecolind.2020.106847>.
- Zheng, Z., Wu, Z., Chen, Y., et al., 2020b. Exploration of eco-environment and urbanization changes in coastal zones: a case study in China over the past 20 years. *Ecol. Indicat.* 119, 106847. <https://doi.org/10.1016/j.ecolind.2020.106847>.